Effect of cycles of electrical stimulation on the contractile performance of engineered heart tissue using human-induced pluripotent stem cell-derived cardiomyocytes

Quinty Halmingh[1]

1 Bachelor Electrical Engineering, University of Twente, Enschede, Overijssel, the Netherlands

Abstract

Engineered Heart Tissue (EHT) is a three-dimensional *in vitro* model that can resemble the cell-cell interaction and tissue organization of the human heart. This *in vitro* model can be patient-specific by using human-induced pluripotent stem cell-derived cardiomyocytes (hiPSC-CMs); however, hiPSC-CMs have shown an immature phenotype which does not resemble the *in vivo* situation. By introducing electromechanical stimulation, the maturation phenotype can be improved, and as a result, higher contractile performance of the hiPSC-CMs can be observed. The optimal electromechanical conditions to improve maturation have not been determined. Therefore, this research focuses on evaluating the effect of different cycles of electrical stimulation on the contractile performance of hiPSC-CMs. Multiple stimulation cycles were tested over a period of five days. The effect induced was evaluated on the physiological level by the change in the force of contraction and spontaneous frequency as well as electrically by the excitation threshold, and current and resistance distribution. This research opened the door to cycles of electrical stimulation on EHTs but further research is necessary to investigate if cycles of electrical stimulation have the potential to improve hiPSC-CMs maturation levels.

Introduction

Cardiovascular diseases (CVDs) remain the predominant cause of death and disability worldwide, with approximately 19 million deaths in 2020. [1] [2]. However, drug development for CVDs is greatly limited by the appearance of adverse drug reactions affecting the heart during clinical studies or after approval. [3] Up to 2013, from the 462 drugs that were withdrawn from the market, 14% were removed due to cardiotoxic side effects. [4]

The main cause of drug-induced cardiotoxic side effects is the inaccurate models that are used for drug screening and development. [5] In pre-clinical studies, animal models are commonly used to evaluate the effect of new compounds, even though they have a limited physiological resemblance to humans. [6] Therefore, there is an urgent need for more appropriate and accurate models that can be used during drug development. [5]

As mentioned by Takahashi et al. (2007), it is possible to generate human-induced pluripotent stem cells, and those can be differentiated into cardiomyocytes. [7] A great advantage of using human-induced pluripotent stem cell-derived cardiomyocytes (hiPSC-CMs) is that these cells can be patient-specific. [7] [8] The 2-dimensional (2D) cardiac

in vitro models made from these hiPSC-CMs are easy to develop and cost-friendly but are unable to recapitulate the cell-cell interactions accurately. [5] [9]

Fortunately, 3-dimensional (3D) cardiac *in vitro* models like Engineered Heart Tissue (EHT) are more advanced in mimicking the *in vivo* behavior of the human heart. [9] [10] EHTs accurately represent the cell-cell interaction and micro-environment [9] [10] and can be fabricated in a versatile platform such as the one developed by Ribeiro et al. (2022). [11] This platform allows to make EHTs in a 12-well plate format which facilitates the maintenance and analysis. [11] The tissues form around two pillars that create mechanical resistance to the tissue. This resistance resembles the mechanical load of the *in vivo* situation. [5]

Nevertheless, the hiPSC-CMs used to make the EHTs have an immature phenotype, corresponding to 16 weeks of fetal development [12], which limits its application for drug development. [5] [10] [13]

A method that promotes the maturation of hiPSC-CMs is electromechanical stimulation. [5] [14] [15] [16] The improvement in the maturation can be observed by a higher contractile performance of the hiPSC-CMs and improved tissue organization. [14] [17] [18] Zhao et al. (2020) investigated ramp stimulation and compared daily increments of 0.2Hz to weekly increments of 1Hz. [14] In both conditions, contractility improvements were observed, but the preference was given to 1Hz. [14] In the study of Ronaldson-Bouchard et al. (2018), constant stimulation of 2Hz was compared to ramp stimulation with increments of 0.33Hz from 2Hz to 6Hz followed by 7 days of 2Hz stimulation. [16] Maturation was claimed for the ramp stimulation group. [16] However, these results have not been able to be replicated in-house with the platform of Ribeiro et al. (2022). [11]

As a consequence, to find the optimal protocol of electrical stimulation that improves maturation in hiPSC-CMs, we have looked at the approach taken with skeletal muscle cells. Valero-Breton et al. (2020) used a 2D configuration and found that repeating a stimulation protocol for multiple days with a long recovery period between sessions was more effective than single-time stimulation. [19] Furthermore, Tarum et al. (2017) found that the same restitution period after pacing showed bigger improvements than a shorter resting period. [20]

Here, we hypothesize that cycles of electrical stimulation, including rest, will improve the contractile performance of EHTs. This paper evaluates the effect of cycles of electrical stimulation on the physiological level by the change in the force of contraction and spontaneous frequency, as well as electrically, by the excitation threshold, and current and resistance distribution.

Materials and methods

EHT platform

The previously designed versatile platform from Ribeiro et al. (2022) was used to make and stimulate EHTs in a 12-well plate format. [11] The platform has 12 holders made from poly(methyl methacrylate; PMMA), each containing one plastic piece holding six pillars. The EHTs form around two pillars so that three EHTs fit into one well and, consequently, 36 tissues in a single plate. The pillars are 3mm in length, and each well contains a working volume of 2mL. [11] More details about the platform are described in [11].

Each holder contains two rectangular-shaped holes for electrodes. The electrodes are perpendicular to the EHTs creating a uniform electric field as shown in Fig. 1A. [11] Here, carbon electrodes were used as their high resistance makes them less sensitive to corrosion. [21] Furthermore, carbon electrodes are capable of transferring change easily. [21] The set-up can be found in S1 Fig.

EHT fabrication and refreshment

The EHTs were made following the protocol published by Ribeiro et al. [11] Briefly, frozen hiPSC-CMs from the WTC lines (GM25256*G0002) were used in combination with 3% human adult cardiac fibroblast (HFB). The HFB were obtained from Promocell (C-12375). The cell mixture was pipetted each well of the 12-well plate. In each well, three slots with the tissue shape were previously made. The plastic pillars were aligned with the holder and allocated into each well. Each tissue is formed from approximately 250.000 cells. After 10 minutes of tissue formation, 1mL of cell medium (Low Insulin, Triiode-L-Thyronine (1:15000), Dexamethasone (1:10000), Insulin-Like Growth factor (1:10000), Lactate (1:1392,8), Glucose (1:100), and Fibroblast Growth Factor (1:5000)) was added. After, the platform was placed in the incubator at 37°C and 10% CO_2.

1mL of cell culture medium was refreshed every other day until the day before the experiment. From then on, the tissues were transferred to a new 12-well plate with 2mL of fresh cell culture medium every 24 hours.

Electrical Stimulation

The tissues were provided with electrical stimulation by a Multi Channel System STG 4008 stimulus generator. [22] The Multi Channel System STG 4008 stimulus generator output biphasic square waves of $32V_{pp}$ and a duration of 2ms for all conditions. [22]

Cycles of electrical stimulation

The cycles of electrical stimulation were divided in two, according to the time of tissue formation, and are defined as late-stage stimulation (stimulation from day 11 until day 16) and early-stage stimulation (stimulation from day 6 until day 10).

Late-stage stimulation applied the following cycles regimes: (i) control; (ii) continuous stimulation (1.2Hz); (iii) 2 hours of stimulation followed by 2 hours rest (2.5Hz) (hereafter cycle (2h/2h)); (iv) 24 hours of stimulation followed by 24 hours rest (2.5Hz)(hereafter cycle (24h/24h)); and (v) 8 hours stimulation followed by 16 hours rest (2.5Hz) (hereafter cycle (8h/16h)).

Contrary, early-stage stimulation applied cycles regimes: (i) control; (ii) continuous stimulation (1.2Hz); (iii) 2 hours of stimulation followed by 2 hours rest (2.5Hz) (hereafter cycle (2h/2h)); (iv) 5 minutes stimulation followed by 10 minutes rest (2.5Hz)(hereafter cycle (5m/10m)); and (v) 8 hours stimulation followed by 16 hours rest (2.5Hz) (hereafter cycle (8h/16h)). An overview of the cycles is presented in Fig. 1B.

Excitation Threshold and Maximum Capture Rate

The excitation threshold (ET) for each tissue was determined by applying biphasic square pulses of 2ms, 2Hz, with a custom-made device. The device allowed a field range from 2.5V/cm to 25V/cm. The pacing was started at 2.5V/cm, and increments of 2.5V/cm were applied until the tissue showed synchronized beating of 2Hz. Once the ET was determined, a 5-second video was recorded. This video was taken by a Nikon Ti2-E inverted microscope with a high-speed camera Prime BSI produced by Photometrics at 100 fps with 2X magnification. [23] The ETs and corresponding currents were measured daily. On the last day, the maximum capture rate (MCR) was measured by stimulating the tissues from 3 to 6Hz. The MCR was set to be 150% and was measured after determining the ETs for all tissues in a well.

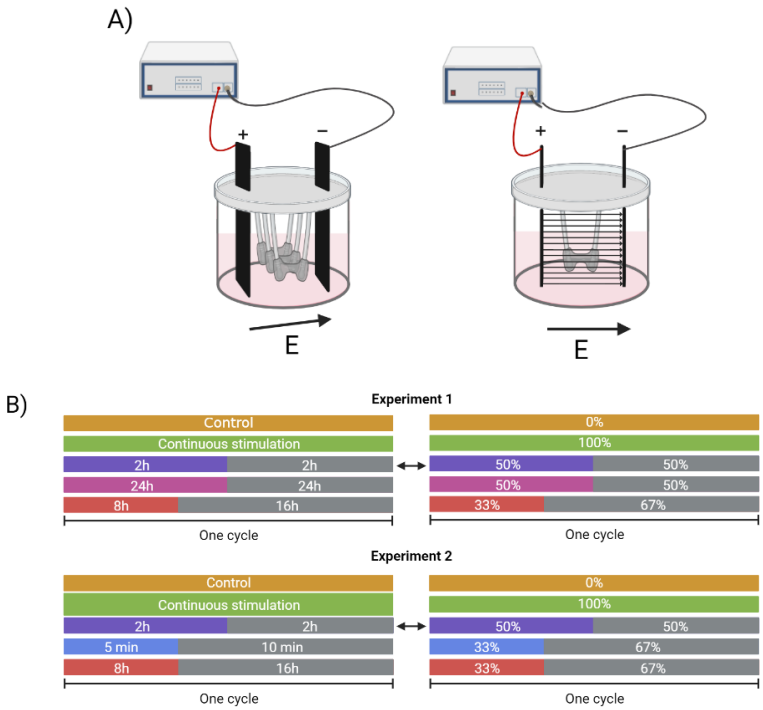

Fig 1. EHT model and cycles of electrical stimulation.
(A). Graphical representation of one well of the 12-well plate platform with the carbon electrodes (left) and representation of the electrical field (right). **(B)**. An overview of the cycles of stimulation of late-stage stimulation and early-stage stimulation. An equivalent representation is presented as percentages of electrical stimulation versus resting time for one cycle of stimulation. Created with BioRender.com

Contractile performance assessment

The contractile performance was measured using a Nikon Ti2-E inverted microscope as previously described with temperature and humidity control (37°C and 10% CO_2). Before measurements, the electrical stimulation was stopped. First, the spontaneous contraction was measured in all the wells, followed by the contraction force under electrical stimulation at 2Hz.

Directly after measuring, the cell culture medium was refreshed as described above. The recorded videos were analysed with software tool *EHT Analysis*, which provided a detailed analysis of different contractile parameters as described in Rivera-Arbeláez et al. (2022). [23] Furthermore, the resistance per well was calculated by the obtained ETs and currents. The timeline of the experiment is presented in Fig. 2.

pH measurement

The pH of the cell culture medium was measured daily to assess the effect of the different cycles of electrical stimulation on the pH. With the use of a Mettler Toledo FiveEasy Plus, the pH values were measured in a 12-well plate after being in the incubator at 37°C and 10% CO_2. The reference cell culture medium was measured after being in the incubator for 3 hours. The other cell culture media used throughout the experiments were put in the incubator overnight and measured the following day.

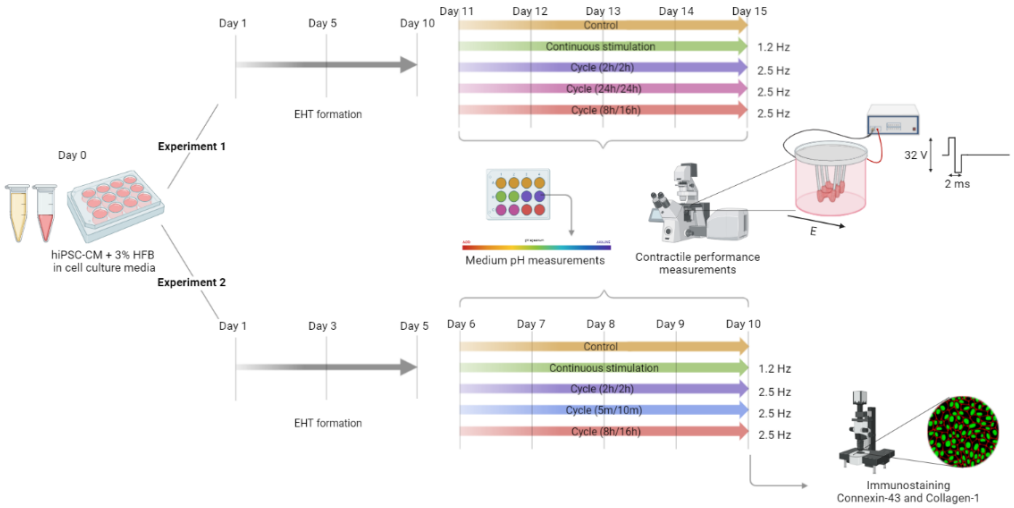

Fig 2. Experiment flow chart.
A schematic timeline of late-stage and early-stage stimulation in parallel. The EHTs were made from hiPSC-CM and HFB, put in cell culture medium, and kept in the incubator at 37°C and 10% CO_2. The tissue formation takes 10 days in late-stage stimulation and 5 days in early-stage stimulation. Electrical stimulation was started on days 11 and 6, respectively. The conditions visible on the arrows are: control (brown), continuous stimulation (green), cycle (2h/2h) (purple), cycle (24h/24h) (pink), cycle (8h/16h) (red), and cycle (5m/10m) (blue). The contractile performance and pH were measured every 24 hours. Immunostaining was done for early-stage stimulation after day 10. Created with BioRender.com

Immunostaining

To observe possible changes in bio-markers connexin-43 (Cx-43) and collagen type 1 (COL1), the EHTs that were early-stage stimulated were subject to immunostaining. First, the EHTs were washed with Dulbecco's Phosphate Buffered Saline (PBS), then fixated with 4% Formaldehyde (FA) for 1 hour. Washings (3 x 20 min) followed, and after the tissues were put in the fridge at 4°C.

20 days later, the tissues were put in a blocking buffer (PBS including 3% Bovine Serum Albumin (BSA), 0.3% Triton, and 0.1% Tween). The following day, the blocking buffer was aspirated and the tissues were transferred to a 96-well plate. Antibody buffer (PBS with 0.1% BSA, 0.3% Triton, and 0.1% Tween) with diluted antibodies was added and the plate was kept at 4°C. In this experiment, the diluted antibodies consist of Cx-43 rabbit (1/250; Sigma-Aldrich, C6219 [24]) with α-actinin mouse (1/800; Sigma-Aldrich, A7811 [25]) and COL1 rabbit (1/200; Novus Biologicals, NB600-408 [26]) with α-actinin mouse (1/800; Sigma-Aldrich, A7811 [25]).

After two days, the tissues were washed in permeabilization buffer (PBS with 0.3% Triton) (3 x 20 min). Antibody buffer (PBS with 0.1% BSA, 0.3% Triton, and 0.1% Tween) was added with diluted secondary antibodies Donkey-anti-Mouse Alexa Fluor 647 (1/500; Thermofisher, A31571 [27]) and Alexa Fluor 488 Chicken a Rabbit (1/500; Thermofisher, A21441 [28]). From this moment forward, the well plate was kept dark.

Lastly, the next day, the EHTs were washed with permeabilization buffer (PBS with 0.3% Triton) (3 x 20 min). DAPI (1/3000; Molecular Probes, D1306 [29]) was added during the first wash.

Results

Electrical conditions

The stimulation pulses were chosen in accordance with the characteristics of the native myocardium; that is, rectangular-shaped pulses 2ms, to resemble the *in vivo* situation [30] [31] [32]

We investigate the role of pacing frequency and rest. First, a condition of continuous stimulation was defined at 1.2Hz (72bpm) to resemble the heartbeat of humans at rest. [33] The stimulation cycles with a restitution period were paced at 2.5Hz (150bpm) corresponding to heart beat while exercising [33].

Late-stage stimulation

The EHTs highest contractile performance was found to be day 10 of tissue formation, as described in Ribeiro et al. (2022). [11] Taking this into account, the tissues in this experiment are stimulated from day 11 to day 15. Therefore, this experiment was named late-stage stimulation.

The contractile performance was measured from day 11 until day 15 and the results are shown in Fig. 3. After one day of stimulation, all conditions show a negative relative change of spontaneous contraction force (Fig. A). The control group showed the highest percentage of increase in spontaneous contraction force on day 15 compared to day 11. And together with continuous stimulation and cycle (8h/16h), the percentage of change in spontaneous contraction force on day 15 is positive relative to day 11. The absolute values show the same positive development for these three conditions (S2 FigA). Besides, cycle (24h/24h) has lower absolute values for spontaneous contraction force than continuous stimulation and all other conditions.

The spontaneous frequency of all conditions became lower over time (Fig. B). The control group was the first to collectively follow 2Hz from day 12. The tissues stimulated with cycle (24h/24h) followed 2Hz collectively from day 14, the other conditions from day 13 as shown in Tab. 1.

The ETs at day 15 were found to be lower than at the start of the experiment for the control group, continuous stimulation, and cycle (8h/16h) (Fig. D). This trend is also observed in the current distribution, and consequently, the resistance of the well remains mainly stable (Fig. E and F). Lastly, on day 15, none of the EHTs were able to follow 4Hz or higher. All EHTs with cycle (24h/24h) were also unable to follow 3Hz, as presented in S1 Table. S3Fig contains two videos of tissues following 2 and 3Hz. Both the absolute values of and change in contraction force during pacing show similar behavior as the spontaneous contraction forces (Fig. E and S2 FigB).

Since the condition cycle (24h/24h) showed the least improvement in contractile performance, it was decided to replace this condition. It seems that the tissues could not recover from elongated stimulation with high frequency. Furthermore, tissues seemed to benefit from a longer restitution period, as observed in cycle (8h/16h). Therefore, that condition was modified to a short cycle of stimulation, namely, cycle (5m/10m) in the early stage of stimulation.

Early-stage stimulation

The EHTs in early-stage stimulation had a shorter period of tissue formation before electrical stimulation started than late-stage stimulation. Again, with the reference point being day 10, therefore called this experiment is called early-stage stimulation. This moment in time was chosen to be able to research the difference in contractile performance between early and late stimulation for cycles of electrical stimulation.

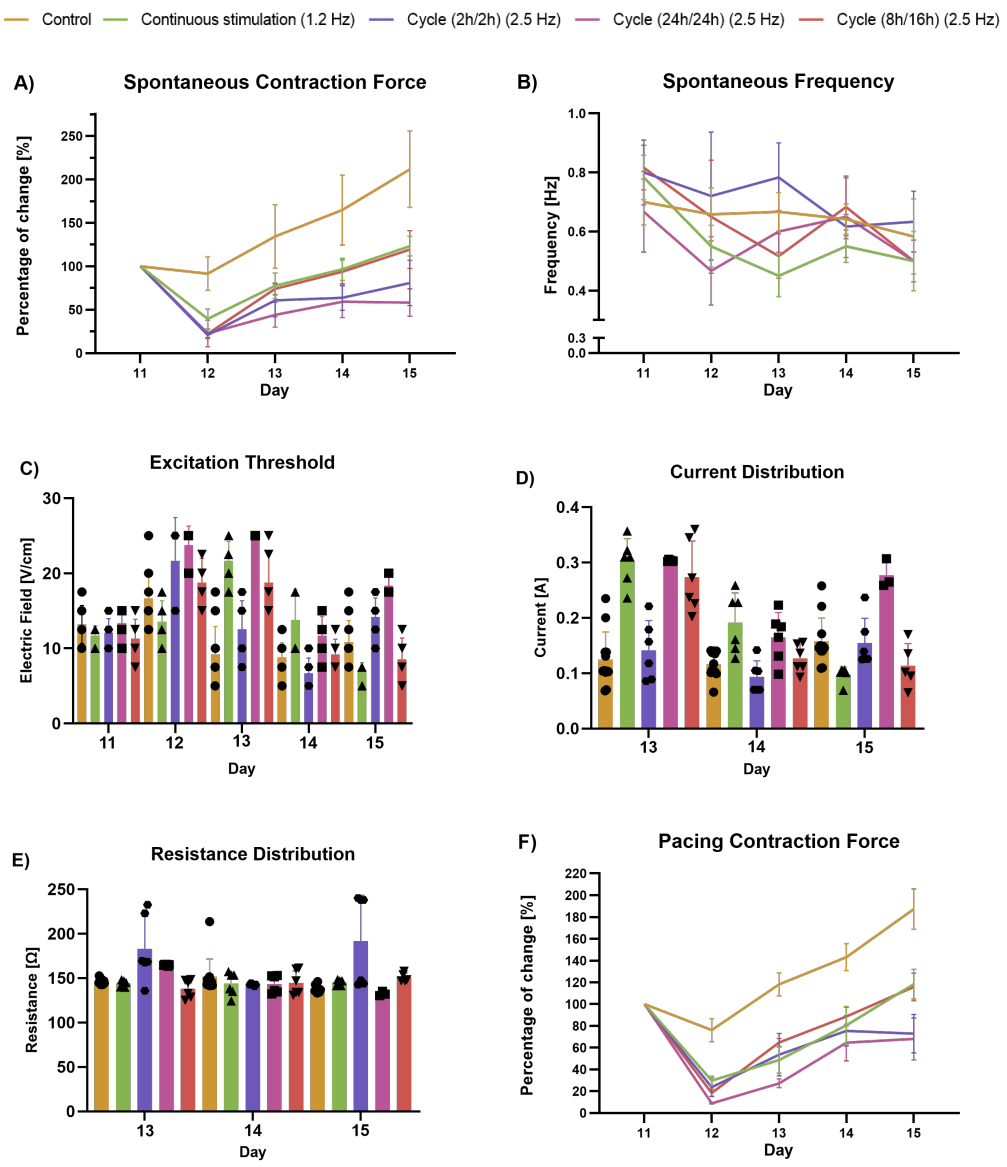

Fig 3. Effect of late-stage of electrical stimulation on contractile performance and electrical conditions.
Contractile performance of EHTs from day 11 until day 15 with multiple cycles of electrical stimulation: control (brown), continuous stimulation with 1.2Hz (green), cycle (2h/2h) with 2.5Hz (purple), cycle (24h/24h) with 2.5Hz (pink), and cycle (8h/16h) with 2.5Hz (red). **(A)**. Relative change of spontaneous force of contraction. **(B)**. Spontaneous frequency. **(C)**. Excitation Threshold. **(D)**. Current distribution. **(E)**.Resistance distribution. **(F)**. Relative change of force of contraction while stimulated. Values are expressed as mean ± SD (N = 1).

In addition to what was mentioned in the EHT fabrication and refreshment section, during this experiment, the electrodes were replaced on day 8.

The results of the contractile performance were observed from day 6 until day 10 and are shown in Fig. 4. All conditions display a positive relation between spontaneous contraction force between day 6 and day 10 (Fig. A). Interestingly, the EHTs that

Table 1. Late-stage stimulation with input frequency 2Hz.
Percentage of tissues following 2Hz per day during late-stage stimulation.

Late-stage stimulation					
	Day 11	*Day 12*	*Day 13*	*Day 14*	*Day 15*
Control	92%	100%	100%	100%	100%
continuous stimulation	100%	83%	100%	100%	100%
2h/2h	100%	67%	100%	100%	100%
24h/24h	100%	67%	50%	100%	100%
8h/16h	100%	50%	100%	100%	100%

were constantly stimulated, reach approximately the same percentage of increase of spontaneous contraction force as the control group at the end of the experiment. Although in terms of absolute values, continuous stimulation reaches lower values than the control group (S4 FigA). Besides, cycle (8h/16h) also reaches higher absolute values than continuous stimulation (S4 FigA). Furthermore, cycle (5m/10m) and cycle (2h/2h) show limited improvements between days 8 and 10 in both relative change and absolute values of spontaneous contraction force.

All conditions show a declining line over time for the spontaneous frequency (Fig. B). Limited synchronized beating was observed throughout the experiment (Tab. 2). Only for the control group and continuous stimulation an ascending trend in percentage of tissues following 2Hz is observed over time. The other conditions were best able to follow on day 8. From then on, fewer tissues could follow 2Hz. Consequently, no EHT was able to follow any frequency above 2Hz (S2 Table).

There is no clear indication of lowered ETs for any of the conditions (Fig. C). A similar current distribution is presented in Fig. D; therefore, the resistance distribution is stable (Fig. E). All conditions show an improvement in percentage of change in pacing contraction force on day 10 compared to day 6 (Fig. F). The percentage increase for contraction force is highest for the control group on day 10 relative to day 6. On day 10, only the control group and continuous stimulation showed positive development in paced contraction force compared to day 8. In terms of absolute values, cycle (2h/2h) comes close to the control group (S4 FigB).

Table 2. Early-stage stimulation with input frequency 2Hz.
Percentage of tissues following 2Hz per day during early-stage stimulation.

Early-stage stimulation					
	Day 6	*Day 7*	*Day 8*	*Day 9*	*Day 10*
Control	100%	42%	47%	79%	74%
continuous stimulation	100%	42%	67%	50%	83%
2h/2h	100%	55%	73%	55%	55%
5min/10min	92%	67%	100%	58%	58%
8h/16h	100%	64%	82%	64%	45%

pH

The results of the pH measurements are presented in S5 Fig including the reference pH *in vivo*. [34] All conditions in late-stage stimulation shows a significant decrease from day 13 onward compared to days 11 and 12. (S5 FigA). After that, the pH values of every condition fluctuate a little, but all remain within the range of 7.5-7.9. The conditions in early-stage stimulation do not show such results (S5 FigB). Here, all conditions are in the same range, and the highest pH value measured does not exceed 7.9.

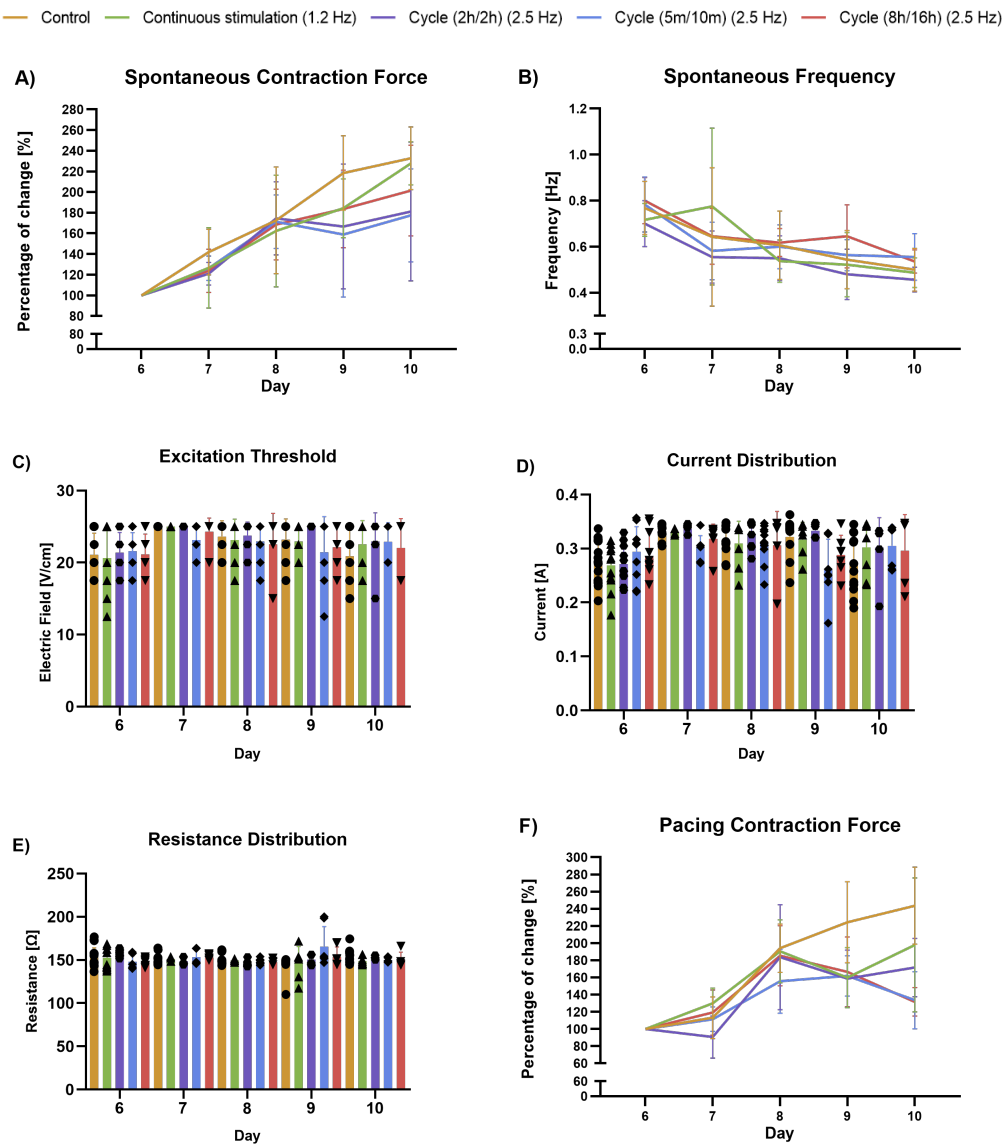

Fig 4. Effect of early-stage of electrical stimulation on contractile performance and electrical conditions.
Contractile performance of EHTs from day 6 until day 10 with multiple cycles of electrical stimulation: control (brown), continuous stimulation with 1.2Hz (green), cycle (2h/2h) with 2.5Hz (purple), cycle (5m/10m) with 2.5Hz (blue), and cycle (8h/16h) with 2.5Hz (red). **(A)**. Relative change of spontaneous force of contraction. **(B)**. Spontaneous frequency. **(C)**. Excitation Threshold. **(D)**. Current distribution. **(E)**. Resistance distribution. **(F)**. Relative change of force of contraction while stimulated. Values are expressed as mean ± SD (N = 2).

Immunostaining

Immunostainings were performed on the early-stage stimulation group to determine the effect of cycles of electrical stimulation on the tissue organization and expressions of bio-markers.

The expression of COL1 was evaluated to determine the presence of fibrotic areas as

a consequence of the cycles of electrical stimulation. No differences were visible between the conditions and the control group (Fig. 5A-E).

Furthermore, the expression of Cx-43 was analyzed, and the results are presented in Fig. 5F-J. In any of the conditions an increase on the expression was observed compared to the control.

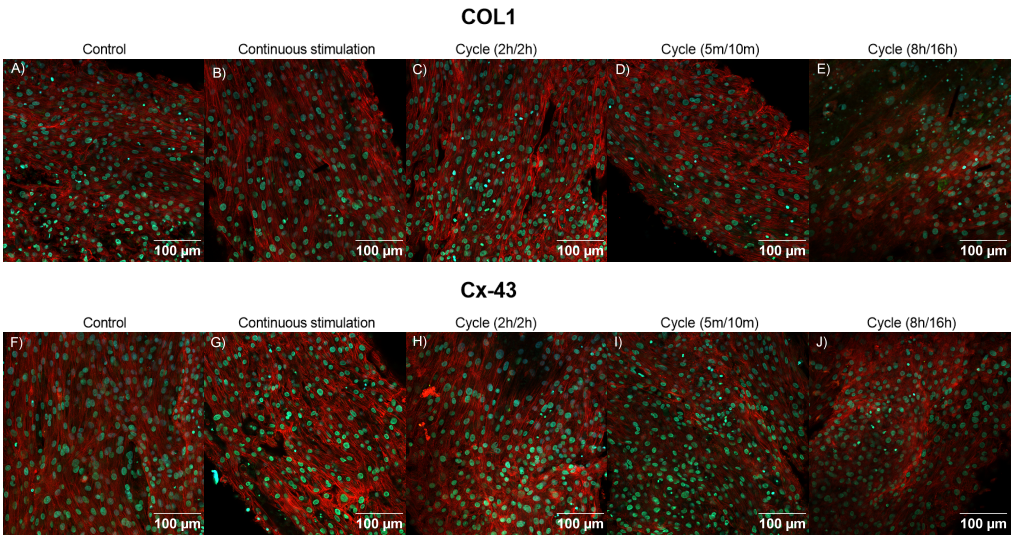

Fig 5. Immunostaining early-stage stimulation.
Confocal images with stained hiPSCM-CMs. α-actinin (red), DAPI (nuclei, blue), with in top panel COL1 (green), and bottom panel Cx-43 (green). Scale bar: 100 μm. **(A&F)**. Control. **(B&G)**. Continuous stimulation with 1.2Hz. **(C&H)**. Cycle (2h/2h) with 2.5Hz. **(D&I)**. Cycle (5m/10m) with 2.5Hz. **(E&J)**. Cycle (8h/16h) with 2.5Hz. Color balance is adjusted with ImageJ for presentation purposes.

Discussion

EHT made from hiPSC-CMs is a 3D *in vitro* model holding great potential for drug development. [10] Zhao et al. (2020) and Ronaldson-Bouchard et al. (2018) showed that electromechanical stimulation can improve the immature phenotype of hiPSC-CMs. [14] [16] However, in-house, the results from Ronaldson-Bouchard et al. (2018) could not be replicated with the EHT platform from Ribeiro et al. (2022). [11] In skeletal muscles, repetitive cycles of electrical stimulation in combination with rest were shown to be effective. [19] [20] Therefore, here, the electrical stimulation conditions were designed based on the results of electrical stimulation on skeletal muscle cells. The effect of different cycles of electrical stimulation at different time points of tissue formation (early or late) was studied in detail.

An important observation during this study is the inability of the tissues to follow the input frequency of 2Hz during early-stage stimulation. (Tab. 1 and Tab. 2). Key differences between immature and mature hiPSC-CM may be linked to the electrophysiology; slower upstroke velocity, shorter plateau phase, and less negative active potential. [35] During the plateau phase, here the pulse duration, calcium enters the cells, which is crucial to couple electrical excitation to physical muscle contraction. [36] The small number of tissues following 2Hz in early-stage stimulation could be caused by the lack of calcium present in the cells and/or the little time for tissue formation. The latter was

already pointed out by Ribeiro et al. (2022). [11]

Since calcium plays a key role in muscle contraction, in future experiments that evaluate contractile performance, one could take into account the calcium concentration in the cells before and throughout the experiment. The cells must contain a sufficient calcium level to be able to follow the input frequency. As this was not achieved with a 2ms duration during early-stage stimulation, one could consider prolonging the pulse duration to force synchronized beating. This suggestion was shortly tested during the early-stage stimulation experiment. After regular measurements on day 7, 29 tissues were stimulated with a pulse duration of 5 and 10ms. Here we found that a total of 86% followed 2Hz with a pulse duration of 5ms while only 31% of the 29 tissues were able to follow 2Hz with 2ms. From the remaining 14%, 100% followed 2Hz with 10ms. Based on these results, a pulse duration of 5ms would be suggested for future experiments using early-stage stimulation.

Multiple parameters were looked at to evaluate the contractile performance of the EHTs. Between experiments, the EHTs in early-stage stimulation showed the biggest improvement in force of contraction both spontaneously and paced (Fig. 3A&F and Fig. 4A&F). Contrary, no significant difference in spontaneous frequency is observed among experiments (Fig. 3B and Fig. 4B). Overall, on the physiological level, early-stage stimulation showed the biggest improvements in contractility.

In late-stage stimulation, the tissues can follow stimulation of 2Hz for lower ETs than with early-stage stimulation (Fig. 3C and Fig. 4C). The average resistance in both experiments is slightly under 150Ω (Fig. 3E and 4E), which is higher in magnitude but in the same order as the average heart resistance of a dead heart which is 97Ω found by Beattie et al. (1953). [37] The least tissues were able to follow 2Hz in early-stage stimulation and only in late-stage stimulation some tissues were able to follow 3Hz (S1 Table and S2 Table). Overall, electrically speaking, during late-stage stimulation more improvement could be observed.

In both experiments, the EHTs that were continuously stimulated showed more improvements in contractile parameters than cycles of electrical stimulation. However, even this condition did not reach the same the levels of contractility as the control group. Since the EHTs of the control group are immature, we conclude that in this study, electrical stimulation did not promote maturation.

In the future, further optimization needs to be done to evaluate if cycles of electrical stimulation could improve maturation. One suggestion would be to extend the stimulation period to, for example, day 6 until day 15. With this, the effect of cycles of electrical stimulation can be evaluated over a longer period, and the results can easily be compared to the data in this paper. Another point one could look into to is the pacing frequency of the cycles. Since continuous stimulation of 1.2Hz showed the best contractility levels of any of the conditions, lower frequency could potentially be beneficial as well to the cycle conditions. Lastly, the determination of the cycles could be explored. The cycle that seemed to best improve was cycle (8h/16h). Therefore future researchers could decide to explore protocols that contain longer periods of pacing and double the resting period.

To improve the platform from Ribeiro et al. (2022), we might look at the high electric field and current values that are applied to the tissues. [11] An easy way to lower these values is by reducing the resistance of the well. Currently, the platform uses a 12-well plate in which the electrodes are distanced 20mm apart. [11] Ribeiro et al. (2022) could innovate by reducing the size of the well and, consequently, reducing the volume of the cell culture medium and shortening the distance between electrodes. Using a smaller well could introduce technical difficulties while fabricating and refreshing the tissues. Therefore, another suggestion would be to look into biohybrid 3D printing similarly to

the work that was done by Yong et al. (2023). [38] Yong et al. (2023) were able to fabricate a platform where the electronics were fully insulated inside PDMS by using carbon black-blended printable PDMS. [38] In the case of Ribeiro et al. (2022), the carbon black-blended printable PDMS could be printed inside the pillars to optimize the distance between the electrodes. Finally, for future experiments where the effect of electrical stimulation is evaluated, it is suggested to only make one tissue per well instead of the 3 technical replicates because it will avoid interference during the different assays like ET or MCR.

The pH is an important parameter to evaluate whether electrical stimulation influences cell functions. [39] As discussed in the results, on the first two days during late-stage stimulation, the pH values for all conditions, including the control group, were relatively high (≈ 8.2) compared to the *in vivo* pH of 7.4. [34] At that point, the pipeline was still being optimized, and a different method was used to measure the pH on these days than described in the method section.

First, the cell culture medium was put in the incubator for 30 min to 1 hour before measurements instead of overnight. The incubator provides CO_2, which stabilizes the pH value of the cell culture medium. It was hypothesized that 30 min to 1 hour was too short for the medium to return to a stable pH after performing measurements. Therefore, from day 13 onward and during early-stage stimulation, the medium was put in the incubator for a longer period. A longer time frame indeed showed a better stabilization of the pH of the cell culture medium (Fig. S5 Fig). Second, the pH on days 11 and 12 was measured from a 50mL falcon tube instead of a 12-well plate. There was one falcon tube per condition, contrary to multiple wells per condition. The reason to switch was to keep the pH measurement conditions equal to the stimulation set-up of the EHTs and ease up the measuring process.

Thus, to evaluate the effect of electrical stimulation on the pH of the cell culture medium, the pH measurement conditions must be equal to the conditions when the EHTs are electrically stimulated. That is, enough CO_2 provided to the cell culture medium and measuring from the initial set-up.

The results of immunostaining showed no observable differences between any of the conditions for COL1 and Cx-43. This would indicate that electrical stimulation did not affect these biomarkers. However, a technicality had likely arisen during the execution of the immunostaining. Both the coloring of COL1 and Cx-43 are almost identical to the DAPI coloring, which is an unexpected result. Instead, more coloring of COL1 and Cx-43 would be expected around nuclei. A plausible cause for these results could be antibody related. It is possible that the primary antibodies were too diluted to show any signal or that the incorrect secondary antibodies were used. Therefore, it is suggested to repeat the immunostaining and include the late-stage group to evaluate if there was an effect in that condition.

To our knowledge, cycles of electrical stimulation to induce maturation in EHTs have not been explored before. Here, we evaluated the effect of repeated cycles, including rest, on different time points of tissue formation. Although maturation was not observed, this study contributes to the development of the ideal conditions of electrical stimulation. And even though a clear improvement compared to the control group was not achieved, we believe that cycles of electrical stimulation still have the potential to improve hiPSC-CMs maturation levels. Although, further research would be necessary to validate this hypothesis.

Conclusion

To conclude, we studied the effect of cycles of electrical stimulation on the contractile performance of EHTs while keeping electrical stimulation and the environmental conditions as physiological as possible. The results showed that cycles of electrical stimulation, including rest, did not reach better levels of contractility than the control group or continuous stimulation. Furthermore, maintaining the physiological situation might not be optimal to reach the desired maturation level, especially when starting electrical stimulation in an early-stage. Nevertheless, the findings of this study are useful for the optimization of the electrical stimulation conditions to induce maturation of the hiPSC-CMs to enable the application EHTs in drug discovery and disease modeling.

Acknowledgement

First, I am most grateful to my chair Prof. Dr. Ir. Loes Segerink for the opportunity to perform this thesis across research groups. I would like to express my great appreciation for my day-to-day supervisor Dr. Ir. José Manual Rivera Arbeláez. Thank you for taking so much time to guide me through my thesis and providing me with extensive feedback. Dr. Verena Schwach, I thank you for taking the time to be a member on my defence committee. I am also grateful to Maureen Dannenberg MSc and Danique Snippert for making the EHTs, helping me with the refreshments and immunostaining, and answering all my lab-related questions. Lastly, I thank AST/BIOS for the great experiences I have had with them the last 12 weeks.

Supporting information

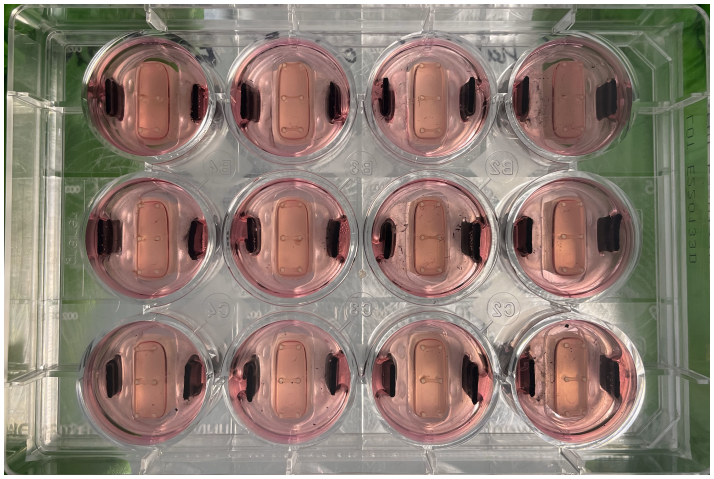

S1 Fig. Bottom view of EHT set-up.

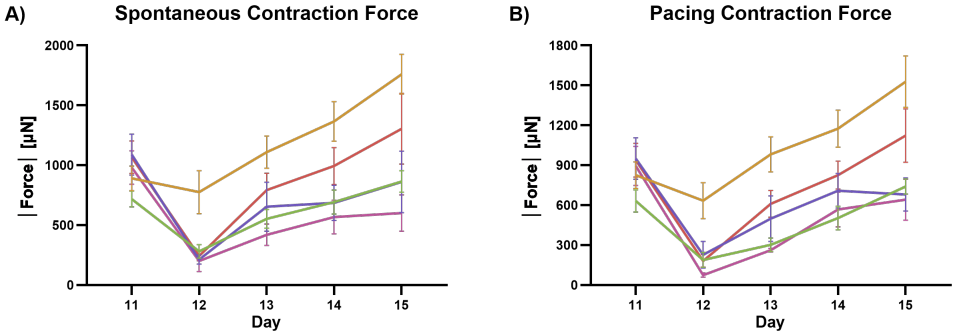

S2 Fig. Absolute force of contraction values of late-stage stimulation. **(A)** Absolute values for spontaneous force of contraction. **(B)** Absolute values for pacing contraction force. Values are expressed as mean ± SD (N = 1).

S1 Table. Maximum Capture Rate late-stage stimulation. MCR of late-stage stimulation. Tissues were paced from 2Hz up to 6Hz with biphasic square pulses of 2ms and 150% ET.

Late-stage stimulation					
	2Hz	*3Hz*	*4Hz*	*5Hz*	*6Hz*
Control	100%	92%	0%	0%	0%
continuous stimulation	100%	33%	0%	0%	0%
2h/2h	100%	67%	0%	0%	0%
24h/24h	100%	0%	0%	0%	0%
8h/16h	100%	50%	0%	0%	0%

A)

B)

S3Fig. Video recordings of EHTs. **(A)** Tissue with frequency 2Hz. **(B)** Tissue with frequency 3Hz.

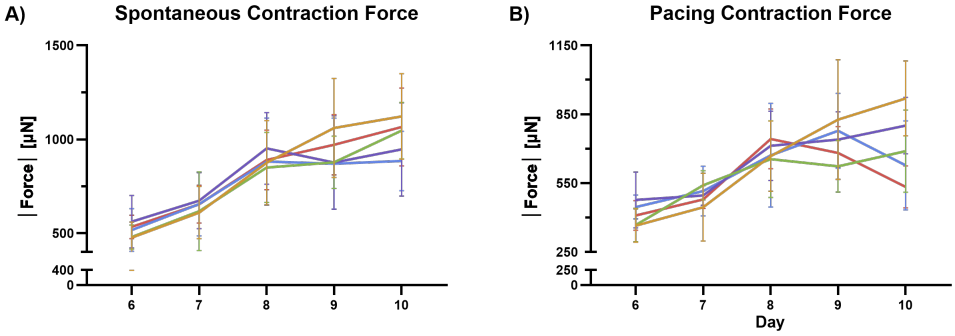

S4 Fig. Absolute force of contraction values of early-stage stimulation. **(A)** Absolute values for spontaneous force of contraction. **(B)** Absolute values for pacing contraction force. Values are expressed as mean ± SD (N = 2).

S2 Table. Maximum Capture Rate early-stage stimulation. MCR of early-stage stimulation. Tissues were paced from 2Hz up to 6Hz with biphasic square pulses of 2ms and 150% ET.

Early-stage stimulation					
	2Hz	*3Hz*	*4Hz*	*5Hz*	*6Hz*
Control	74%	0%	0%	0%	0%
continuous stimulation	83%	0%	0%	0%	0%
2h/2h	55%	0%	0%	0%	0%
5min/10min	58%	0%	0%	0%	0%
8h/16h	45%	0%	0%	0%	0%

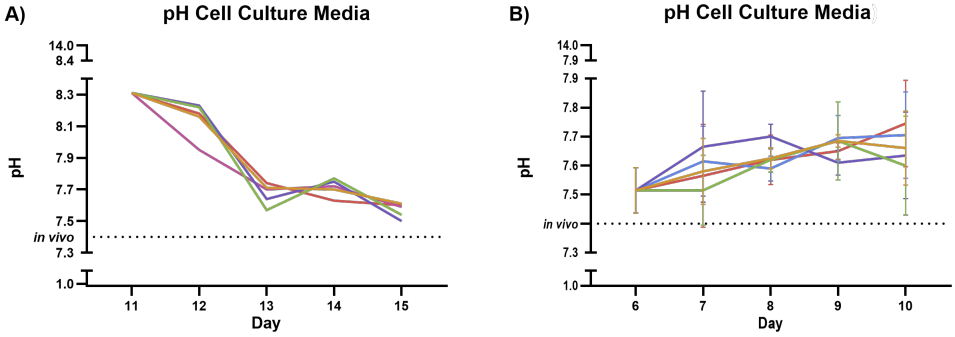

S5 Fig. pH values late-stage stimulation and early-stage stimulation. pH of cell culture medium: control (brown), continuous stimulation with 1.2Hz (green), cycle (2h/2h) with 2.5Hz (purple), cycle (24h/24h) with 2.5Hz (pink), cycle (5m/10m) with 2.5Hz (blue), and cycle (8h/16h) with 2.5Hz (red). **(A)** pH for late-stage stimulation (N = 1). **(B)** pH for early-stage stimulation (N = 2). Values are expressed as mean ± SD.

References

1. Tsao, C. W., Aday, A. W., Almarzooq, Z., Alonso, A., Beaton, A., Bittencourt, M. S., Boehme, A. K., Buxton, A. E., Carson, A. P., Commodore-Mensah, Y., Elkind, M. S., Evenson, K. R., Eze-Nliam, C., Ferguson, J. F., Generoso, G., Ho, J. E., Kalani, R., Khan, S. S., Kissela, B. M., . . . Martin, S. S. (2022). Heart Disease and Stroke Statistics - 2022 Update: A Report From the American Heart Association. *Circulation, 145(8)*. https://doi.org/10.1161/cir.0000000000001052

2. World Health Organization: WHO. (2021). Cardiovascular diseases (CVDs). *www.who.int*. https://www.who.int/news-room/fact-sheets/detail/cardiovascular-diseases-(cvds)

3. Mamoshina, P., Rodriguez, B., & Bueno-Orovio, A. (2021). Toward a broader view of mechanisms of drug cardiotoxicity. *Cell Reports Medicine, 2*(3), 100216. https://doi.org/10.1016/j.xcrm.2021.100216

4. Onakpoya, I., Heneghan, C., & Aronson, J. K. (2016). Post-marketing withdrawal of 462 medicinal products because of adverse drug reactions: a systematic review of the world literature. *BMC Medicine, 14*(1). https://doi.org/10.1186/s12916-016-0553-2

5. Stein, J. M., Mummery, C. L., & Bellin, M. (2021). Engineered models of the human heart: Directions and challenges. *Stem Cell Reports, 16*(9), 2049–2057. https://doi.org/10.1016/j.stemcr.2020.11.013

6. Vanderburgh, J. P., Sterling, J. A., & Guelcher, S. A. (2016). 3D Printing of Tissue Engineered Constructs for In Vitro Modeling of Disease Progression and Drug Screening. *Annals of Biomedical Engineering, 45*(1), 164–179. https://doi.org/10.1007/s10439-016-1640-4

7. Takahashi, K., Tanabe, K., Ohnuki, M., Narita, M., Ichisaka, T., Tomoda, K., & Yamanaka, S. (2007). Induction of Pluripotent Stem Cells from Adult Human Fibroblasts by Defined Factors. *Cell, 131*(5), 861–872. https://doi.org/10.1016/j.cell.2007.11.019

8. Li, M., Peng, L., & Chen, X. (2022). Pharmacogenomics in drug-induced cardiotoxicity: Current status and the future. *Frontiers in Cardiovascular Medicine, 9*. https://doi.org/10.3389/fcvm.2022.966261

   Koivumäki, J. T., Naumenko, N., Tuomainen, T., Takalo, J., Oksanen, M., Puttonen, K. A., Lehtonen, Š., Kuusisto, J., Laakso, M., Koistinaho, J., & Tavi, P. (2018). Structural Immaturity of Human iPSC-Derived Cardiomyocytes: In Silico Investigation of Effects on Function and Disease Modeling. *Frontiers in Physiology, 9*. https://doi.org/10.3389/fphys.2018.00080

9. Abdelsayed, G., Ali, D., Malone, A. F., Saidi, J., Myneni, M., Slepian, M. J., Cheema, F. H., & Hameed, A. (2022). 2D and 3D in-Vitro models for mimicking cardiac physiology. *Applications in Engineering Science, 12*, 100115. https://doi.org/10.1016/j.apples.2022.100115

10. Eder, A., Vollert, I., Hansen, A., & Eschenhagen, T. (2016). Human engineered heart tissue as a model system for drug testing. *Advanced Drug Delivery Reviews, 96*, 214–224. https://doi.org/10.1016/j.addr.2015.05.010

11. Ribeiro, M. L., Rivera-Arbeláez, J. M., Cofiño-Fabres, C., Schwach, V., Slaats, R. H., Den, S. a. T., Vermeul, K., Van Den Berg, A., Pérez-Pomares, J. M., Segerink,

L. I., Guadix, J. A., & Passier, R. (2022). A New Versatile Platform for Assessment of Improved Cardiac Performance in Human-Engineered Heart Tissues. *Journal of Personalized Medicine, 12*(2), 214. https://doi.org/10.3390/jpm12020214

12. Ulmer, B. M., & Eschenhagen, T. (2020). Human pluripotent stem cell-derived cardiomyocytes for studying energy metabolism. *Biochimica Et Biophysica Acta. Molecular Cell Research, 1867*(3), 118471. https://doi.org/10.1016/j.bbamcr.2019.04.001

13. Yang, X., Pabon, L., & Murry, C. E. (2014). Engineering Adolescence. *Circulation Research, 114*(3), 511–523. https://doi.org/10.1161/circresaha.114.300558

14. Zhao, Y., Rafatian, N., Wang, E. Y., Feric, N. T., Lai, B. F., Knee-Walden, E. J., Backx, P. H., & Radisic, M. (2020). Engineering microenvironment for human cardiac tissue assembly in heart-on-a-chip platform. *Matrix Biology, 85–86*, 189–204. https://doi.org/10.1016/j.matbio.2019.04.001

15. Zhang, Y., Aleman, J., Arneri, A., Bersini, S., Piraino, F., Shin, S. R., Dokmeci, M. R., & Khademhosseini, A. (2015). From cardiac tissue engineering to heart-on-a-chip: beating challenges. *Biomedical Materials, 10*(3), 034006. https://doi.org/10.1088/1748-6041/10/3/034006

16. Ronaldson-Bouchard, K., P, S., MA, Yeager, K., Chen, T. F., Song, L., Sirabella, D., Morikawa, K., Teles, D., Yazawa, M., & Vunjak-Novakovic, G. (2018). Advanced maturation of human cardiac tissue grown from pluripotent stem cells. *Nature, 556*(7700), 239–243. https://doi.org/10.1038/s41586-018-0016-3

17. Carlos-Oliveira, M., Lozano-Juan, F., Occhetta, P., Visone, R., & Rasponi, M. (2021). Current strategies of mechanical stimulation for maturation of cardiac microtissues. *Biophysical Reviews, 13*(5), 717–727. https://doi.org/10.1007/s12551-021-00841-6

18. Lundy, S., Zhu, W., Regnier, M., & Laflamme, M. A. (2013). Structural and Functional Maturation of Cardiomyocytes Derived from Human Pluripotent Stem Cells. *Stem Cells and Development, 22*(14), 1991–2002. https://doi.org/10.1089/scd.2012.0490

19. Valero-Breton, M., Warnier, G., Castro-Sepulveda, M., Deldicque, L., & Zbinden-Foncea, H. (2020). Acute and Chronic Effects of High Frequency Electric Pulse Stimulation on the Akt/mTOR Pathway in Human Primary Myotubes. *Frontiers in Bioengineering and Biotechnology, 8*. https://doi.org/10.3389/fbioe.2020.565679

20. Tarum, J., Folkesson, M., Atherton, P. J., & Kadi, F. (2017). Electrical pulse stimulation: an *in vitro* exercise model for the induction of human skeletal muscle cell hypertrophy. A proof-of-concept study. *Experimental Physiology, 102*(11), 1405–1413. https://doi.org/10.1113/ep086581

21. Tandon, N., Cannizzaro, C., Figallo, E., Voldman, J., & Vunjak-Novakovic, G. (2006). *Characterization of Electrical Stimulation Electrodes for Cardiac Tissue Engineering*. https://doi.org/10.1109/iembs.2006.259747

22. Multichannelsystems. (2021). *Stimulus Generator Manual STG 4004 and STG 4008*. `https://www.multichannelsystems.com/sites/multichannelsystems.com/files/documents/manuals/MCS_STG4004%2BSTG4008_Manual.pdf`

23. Rivera-Arbeláez, J. M., Cofiño-Fabres, C., Schwach, V., Boonen, T., Den, S. a. T., Vermeul, K., Van Den Berg, A., Segerink, L. I., Ribeiro, M. L., & Passier, R. (2022). Contractility analysis of human engineered 3D heart tissues by an automatic tracking technique using a standalone application. *PLOS ONE, 17*(4), e0266834. https://doi.org/10.1371/journal.pone.0266834

24. *Anti-Connexin-43 antibody produced in rabbit.* (n.d.). `https://www.sigmaaldrich.com/NL/en/product/sigma/c6219`

25. *Monoclonal Anti-α-Actinin (Sarcomeric) antibody produced in mouse.* (n.d.). `https://www.sigmaaldrich.com/NL/en/product/sigma/a7811`

26. *Collagen I Antibody.* (n.d.). Novus Biologicals. `https://www.novusbio.com/products/collagen-i-antibody_nb600-408`

27. *Donkey anti-Mouse IgG (H+L) Highly Cross-Adsorbed, Alexa FluorTM 647 (A-31571).* (n.d.). `https://www.thermofisher.com/antibody/product/Donkey-anti-Mouse-IgG-H-L-Highly-Cross-Adsorbed-Secondary-Antibody-Polyclonal/A-31571`

28. *Chicken anti-Rabbit IgG (H+L) Cross-Adsorbed, Alexa FluorTM 488 (A-21441).* (n.d.). `https://www.thermofisher.com/antibody/product/Chicken-anti-Rabbit-IgG-H-L-Cross-Adsorbed-Secondary-Antibody-Polyclonal/A-21441`

29. *DAPI (4',6-Diamidino-2-Phenylindole, Dihydrochloride).* (n.d.). `https://www.thermofisher.com/order/catalog/product/D1306`

30. Radisic, M., Park, H., Shing, H., Consi, T. R., Schoen, F. J., Langer, R., Freed, L. E., & Vunjak-Novakovic, G. (2004). Functional assembly of engineered myocardium by electrical stimulation of cardiac myocytes cultured on scaffolds. *Proceedings of the National Academy of Sciences of the United States of America, 101*(52), 18129–18134. https://doi.org/10.1073/pnas.0407817101

31. Stoppel, W. L., Kaplan, D. L., & Black, L. D. (2016). Electrical and mechanical stimulation of cardiac cells and tissue constructs. *Advanced Drug Delivery Reviews, 96*, 135–155. https://doi.org/10.1016/j.addr.2015.07.009

32. Tandon, N., Marsano, A., Maidhof, R., Wan, L. Q., Park, H., & Vunjak-Novakovic, G. (2011). Optimization of electrical stimulation parameters for cardiac tissue engineering. *Journal of Tissue Engineering and Regenerative Medicine, 5*(6), e115–e125. https://doi.org/10.1002/term.377

33. Target Heart Rates Chart. (2023, May 15). `https://www.heart.org/en/healthy-living/fitness/fitness-basics/target-heart-rates`

34. Hopkins, E., Sanvictores, T., & Sharma, S. (2022). *Physiology, acid base balance. In StatPearls [Internet].* StatPearls Publishing.

35. Guo, Y., & Pu, W. T. (2020). Cardiomyocyte Maturation. *Circulation Research, 126*(8), 1086–1106. https://doi.org/10.1161/circresaha.119.315862

36. Grant, A. O. (2009). Cardiac Ion Channels. *Circulation-arrhythmia and Electrophysiology, 2*(2), 185–194. https://doi.org/10.1161/circep.108.789081

37. Beattie, E. J., Keshishian, J. M., Ames, N. B., & Blades, B. (1953). THE ELECTRICAL RESISTANCE OF THE HEART. *Annals of Surgery, 137*(4), 504–506. https://doi.org/10.1097/00000658-195304000-00011

38. Yong, U., Jin, S., Kim, H., Hwang, D. G., Cho, S., Nam, H., Kim, S., Kim, T. Y., Jeong, U., Kim, K., Chung, W. K., Yeo, W., & Jang, J. (2023). Biohybrid 3D Printing of a Tissue-Sensor Platform for Wireless, Real-Time, and Continuous Monitoring of Drug-Induced Cardiotoxicity. *Advanced Materials, 35*(11). https://doi.org/10.1002/adma.202208983

39. [The importance of intracellular pH in the regulation of cell function]. (2003, April 1). PubMed. https://pubmed.ncbi.nlm.nih.gov/12746799/